COMPOSITION AND CHARACTERISTICS OF TRABECULAR BONE IN OSTEOPOROSIS AND OSTEOARTHRITIS

PUBLISHED VERSION:

I Tamimi, ARG Cortes, JM Sanchez, JL Ackerman, D González, A García, F Yaghoubi, MN Abdallah, H Eimar, M Laurenti, A Al-Subaie, E. Guerado, D. Garcia de Quevedo, F Tamimi. Composition and characteristics of trabecular bone in osteoporosis and osteoarthritis . Bone. 2020 Nov:140:115558. DOI: 10.1016/j.bone.2020.115558

AUTHORS:

TAMIMI ISKANDAR

Orthopedic Surgery Consultant, Hospital Regional Universitario de Malaga, Avenida Carlos Haya SN, Malaga, 29010, Spain. Tel: 0034 633308406, email: isktamimi80@yahoo.com, fax 0034 952 901171. ***(Corresponding author).***

ARTHUR RODRIGUEZ GONZALEZ CORTES

Associate Professor, Department of Dental Surgery, Faculty of Dental Surgery, University of Malta. Martinos Center for Biomedical Imaging, Department of Radiology, Massachusetts General Hospital, Charlestown, MA, USA. Department of Radiology, Harvard Medical School, Boston, MA, USA, email: arturodeltoro8@hotmail.com.

JUAN MANUEL SANCHEZ SILES

Orthopedic Surgery Consultant, Hospital Regional Universitario de Malaga, Avenida Carlos Haya SN, Malaga, 29010, Spain. email: jumasansi@gmail.com, fax 0034 952 901171.

JEROME L. ACKERMAN

Associate Professor, Martinos Center for Biomedical Imaging, Department of Radiology, Massachusetts General Hospital, Charlestown, MA, USA. Department of Radiology, Harvard Medical School, Boston, MA, USA. Email: jerry@nmr.mgh.harvard.edu

DAVID GONZALEZ DE QUEVEDO

Orthopedic Surgery Consultant, Hospital Regional Universitario de Malaga, Avenida Carlos Haya SN, Malaga, 29010, Spain. email: deividgq@gmail.com, fax 0034 952 901171.

ANGEL GARCIA

Orthopedic Surgery Nurse, Hospital Regional Universitario de Malaga, Avenida Carlos Haya SN, Malaga, 29010, Spain. email: angelgarciasantos1@gmail.com, fax 0034 952 901171.

FARID YAGHOUBI

Dentistry Student, McGill University, 3640 University Street, Montreal, Canada, H3A 2B2. Tel.: 514-398-7203, Fax: 514-398-8900. email: farid.yaghoubi@gmail.com.

MOHAMED NUR ABDULLAH

Orthodontics and Dentofacial Orthopedics Resident. McGill University, 3640 University Street, Montreal, Canada, H3A 2B2. Tel.: 514-398-7203, Fax: 514-398-8900. mohamed.abdallah@mail.mcgill.ca.

HAZEM EIMAR

Dentistry Resident, Faculty of Medicine and Dentistry, University of Alberta, 2J2.00 WC Mackenzie Health Sciences Centre 8440 112 St. NW Edmonton , Alberta ,Canada T6G 2R7. eimar@ualberta.ca

AMMAR ALSHEGHRI

Orthodontics and Dentofacial Orthopedics Resident. McGill University, 3640 University Street, Montreal, Canada, H3A 2B2. Tel.: 514-398-7203, Fax: 514-398-8900. ammar.alsheghri@mail.mcgill.ca

MARCO LAURENTI

Assistant Professor. Facultad de Farmacia · Departamento de Química en Ciencias Farmacéuticas, Universidad Complutense de Madrid. Spain , marclaur@ucm.es.

AHMAD AL-SUBAEI

PhD Student. McGill University, 3640 University Street, Montreal, Canada, H3A 2B2. Tel.: 514-398-7203, Fax: 514-398-8900. ahmed.alsubaie@mail.mcgill.ca.

DAVID GARCIA DE QUEVEDO

Chief of the Orthopedic Surgery Department, Hospital Regional Universitario de Malaga, Avenida Carlos Haya SN, Malaga, 29010, Spain. email: dgqpsm@gmail.com, fax 0034 952 901171.

ENRIQUE GUERADO

Orthopedic Surgery Professor, Faculty of Medicine, University of Malaga, Bulevar Louis Pasteur, 32, 29010 Málaga, Spain. Tel: 952 13 15 42. eguerado@telefonica.net

TAMIMI FALEH

Associate Professor, Faculty of Dentistry, McGill University, 3640 University Street, Montreal, Canada, H3A 2B2. Tel.: 514-398-7203, Fax: 514-398-8900. faleh.tamimimarino@mcgill.ca.

COMPOSITION AND CHARACTERISTICS OF TRABECULAR BONE IN OSTEOPOROSIS AND OSTEOARTHRITIS

Abstract:

Background: Bone strength depends on multiple factors such as bone density, architecture, and composition turnover. However, the role these factors play in osteoporotic fractures is not well understood.

Purpose: The aim of this study was to analyze trabecular bone architecture, and its crystal and organic composition in humans, by comparing samples taken from patients who had a hip fracture (HF) and individuals with hip osteoarthritis (HO).

Methods: The study included 31 HF patients and 42 cases of HO who underwent joint replacement surgery between 1/1/2013–31/12/2013. Trabecular bone samples were collected from the femoral heads and analyzed using dual-energy X-ray absorptiometry, μ-CT, and solid-state high-resolution magic-angle-spinning nuclear magnetic resonance (MAS-NMR) spectroscopy.

Results: No differences in proton or phosphorus concentration were found between the two groups using ^{1}H single pulse, ^{31}P single pulse, ^{31}P single pulse with proton decoupling NMR spectroscopy, in hydroxyapatite (HA) c-axis or a-axis crystal length. Bone volume fraction (BV/TV), trabecular number (Tb.N), and bone mineral density (BMD) were higher in the HO group than in the HF group [28.6% ± 10.5 vs 20.3% ± 6.6 ($p = 0.026$); 2.58 ± 1.57 mm^{-1} vs 1.5 mm^{-1} ± 0.79 ($p = 0.005$); and 0.39 g/cm^2 ± 0.10 vs. 0.28 g/cm^2 ± 0.05 ($p = 0.002$), respectively]. The trabecular separation (Tb.Sp) was lower in the HO group 0.42 mm ± 0.23 compared with the HF group 0.58 mm ± 0.27 ($p=0.036$).

In the HO group, BMD was correlated with BV/TV ($r = 0.704$, $p = <0.001$), Tb.N ($r = 0.653$; $p = <0.001$), Tb.Sp (-0.561, $p = <0.001$), and ^{1}H concentration (-0.580, $p = <0.001$). BMD was not

correlated with BV/TV, Tb.Sp , Tb.Th, Tb.N, Tb. PF, ^{1}H concentration, or HA crystal size in the HF group.

Conclusions:

Patients with HO who did not sustain previous hip fractures had a higher femoral head BMD, BV/TV, and Tb.N than HF patients. In HO patients, BMD was positively correlated with the BV/TV and Tb.N and negatively correlated with the femoral head organic content and trabecular separation. Interestingly, these correlations were not found in HF patients with relatively lower bone densities. Therefore, osteoporotic patients with similar low bone densities could have significant microstructural differences. No differences were found between the two groups at a HA crystal level.

Keywords: Micro-computed tomography, Nuclear magnetic resonance, femoral head bone fractures, osteoporosis, hydroxyapatite, crystal structure.

MANUSCRIPT:

Introduction:

The strength of a material is a function of the composition of the material as well as its geometric structure described at the macro, micro and nano dimensional scales. In the case of bone, these dimensional scales correspond respectively to the overall bone shape (e.g., cortical thickness), trabecular architecture (e.g., bone volume fraction, trabecular number), and apatite

125 nanocrystalline structure (e.g., crystal size, distribution, structure and chemical composition) [1,
126 2]. Except for mineral content (BMC or BMD), composition has rarely been included in
127 investigations of bone strength. This study uniquely applies a variety of experimental methods to
128 study bone morphology at the micro and nano-structural scales, as well as a variety of
129 compositional parameters.

130 The macro and microstructural features of bone have been extensively studied in the literature
131 using micro-computed tomography scan (μ-CT) analysis and other techniques, suggesting that
132 the trabecular architecture could be an independent factor contributing to bone strength [3–5].
133 The role bone mineral density plays on the mechanical properties of bone has been well
134 stablished, and dual-energy x-ray absorptiometry (DXA) which is the traditionally used method
135 for the diagnosis of osteoporosis, has proven its efficiency in the prediction of hip and vertebral
136 fractures [6]. Although research on bone at the macro- and microstructural levels are routinely
137 carried out, studies at the nanostructural level are scarce.

138 On other hand, x-ray powder diffraction (XRD) is a technique used to analyze the structure of
139 crystalline materials, which gives information on the crystal nanostructure and its chemical
140 composition. XRD has been previously used in the nanostructural analysis of hydroxyapatite
141 (HA) crystals [7]. Solid-state magic-angle-spinning (MAS) spectroscopy is a novel method used
142 to perform experiments in solid-state nuclear magnetic resonance (NMR) spectroscopy and
143 liquid proton nuclear magnetic resonance [8]. It improves the resolution of the analysis by
144 spinning the sample at the magic angle θ with respect to the direction of the magnetic field.
145 Solid-state NMR spectroscopy is a useful tool in the characterization of the organic content of
146 bone and MAS technique permits recording NMR spectra of solid materials [9–11]. The

objective of this study was to examine the nanostructural composition and microstructural features of trabecular femoral head bone in patients undergoing surgery for hip fracture or hip osteoarthritis using XRD, MAS-NMR spectroscopy as well as µ-CT scan, and bone densitometry analyses. In addition, we aimed to analyze the correlation between BMD, which is the current gold standard in the diagnosis of osteoporosis, with other bone micro-and nanostructural parameters of bone trabeculae.

Materials and Methods:

Approvals from our local ethical board and from the Andalusian Public Health System Bio-bank were obtained to conduct this cross-sectional study. Femoral heads were collected from patients who underwent total or partial hip replacement during the period 1/1/2013 – 31/12/2013. The clinical information of the participants was withdrawn from the computerized database of the Orthopedic Surgery Department without any exposure of personal information. We included samples taken from individuals who were operated for the treatment of either osteoporotic intracapsular hip fractures, or hip osteoarthritis (with no previous hip fractures). Patients with high energy fractures as well as pathological fractures (i.e., secondary to osteomalacia, Paget´s disease, primary bone tumors or bone metastasis), or diagnosed with avascular necrosis of the femoral head, were excluded from the analysis. The following parameters were retrieved from patients´ files and computerized records: age, gender, fracture side, body mass index (BMI), information on drug intake, history of smoking and alcohol consumption. The general health status was estimated using the age-factored Charlson comorbidity score [12].

Sample preparation:

The femoral heads were harvested during standard total hip and partial hip replacement procedures. An awl was used to withdraw 1.0 cm Ø x 1.5 cm cylindrical bone samples from the weight bearing area of the femoral head, 1.0 cm above the fovea (Figure 1). The bone samples were then placed in a 10% formaldehyde solution and stored at 4° C. A 2.0 mm^3 bone fragment was then collected from the distal end of each sample, using a 1.0 Ø mm cylindrical burr adapted to a handpiece drill (Stryker, Hamilton, ON). Then, each fragment was cleaned with three 60 minute cycles of de-ionized distilled water at 25°C, followed by three cycles of dehydration and defatting with 100% alcohol for 60 minutes [13]. Finally, the bone samples were powdered using a ceramic pestle, and the resulting powder transferred to separate sample tubes and stored at 4°C.

Bone densitometry:

Bone density was analyzed using a bone densitometry device (GE Lunar PIXImus) with a focal spot size of 0.25 x 0.25 mm, an image area of 100 x 80 mm, current of 400 µA, and energy of 80 kV. The region of interest (ROI) was established 10.0 mm deep from the articular surface, to avoid subchondral bone. The following parameters were measured: bone mineral content (BMC, ratio between the mineral weight and the dry weight of the bone sample), and bone mineral density (BMD, is the amount of bone mineral in bone tissue).

Micro-computed tomography:

The structural characteristics of the bone samples were analyzed using a µ-CT (SkyScan1172; SkyScan; Kontich, Belgium) with a voltage of 80 kV, current of 120 µA, a resolution of 10.88

μm, an aluminum filter of 0.5 mm thickness, and a rotation step of 0.5 degrees. The ROI included trabecular bone from 5.0 to 10.0 mm deep from the articular surface, selected to bypass sclerotic areas or subchondral cysts (Figure 1). The following features were then measured: trabecular number (Tb.N, reflects the number of trabeculae within the region of interest), trabecular separation (Tb.Sp, measures the space between the trabeculae), trabecular pattern factor (Tb.Pf, quantifies the connectedness between the trabeculae), bone volume fraction (BV/TV, the percentage of bone in relation the total volume) , and trabecular thickness (Tb.Th, reflects the size of the trabeculae) .

X-ray powder diffraction:

The hydroxyapatite (HA) crystals were analyzed using an XRD device (D8-Discover/GADDS, Bruker, Karlsruhe, Germany). The diffractometer with CuKα radiation (setting: 40 kV, 40 mA, Theta1 15°, Theta2 15° scanning angle, frame width 23°, mode STEP and 1800 scan step time) was used to record the XRD [14]. Data from each XRD spectrum were analyzed using A DIFFRAC-plus EVA software (AXS, Bruker, Karlsruhe, Germany) [15].

The average HA a-axis and c-axis crystal lengths were calculated for each bone sample using Scherrer's formula (Eq. 1) and the (310) and (002) Bragg peaks of the XRD spectrum. In general the HA crystal size increases both along the c and a axes [16]. K is the shape factor, D is the average of domain lengths, λ is the x-ray wavelength, β is the line broadening at half the maximum intensity (FWHM) and θ is the Bragg angle:

$$D = K\lambda/\beta\cos\theta \quad (1)$$

Solid-state magic-angle-spinning nuclear magnetic resonance spectroscopy:

MAS-NMR spectroscopy was used to analyze the chemical composition of the powdered bone samples. This is a well-established technique used in the compositional analysis of solid materials [17]. Measurements were obtained using a Bruker (Billerica, MA) AVANCE NMR spectrometer, equipped with a Magnex (Oxford, UK) 14 Tesla field strength magnet, yielding phosphorus and proton frequencies of 242.94 and 600.13 MHz, respectively. We used a Bruker solid-state CPMAS cross-polarization magic-angle-spinning) probe with B_1 fields of 70–80 kHz (40 kHz for CP) to obtain solid-state ^{31}P spectra with a single 90º pulse and with proton decoupling at a sample rotation speed of 2.5 kHz. All measurements performed on the powdered bone samples were immediately consecutive, to prevent potential tuning changes of the spectrometer. Measurements were stratified by the weight of the power, into four different variables: (1) phosphorus relative concentration measured with $^{1}H/^{31}P$ cross-polarization NMR spectroscopy, (2) hydrogen relative concentration measured with ^{1}H single pulse NMR spectroscopy, (3) phosphorus relative concentration measured with ^{31}P single pulse NMR spectroscopy, and (4) phosphorus relative concentration measured with ^{31}P single pulse with proton decoupling NMR spectroscopy. These concentrations are denoted as “relative” because they are dimensionless quantities relative to each other but are not referenced to an absolute concentration unit such as g/cm2. The ^{1}H, ^{31}P, and ^{31}P with proton decoupling measurements reflect the organic matrix content, the overall mineral content, and the mineral content of the interior of the apatite nanocrystals respectively; the last quantity factors in the size of the nanocrystals [10, 11, 17, 18]. The organic matrix constitutes about 40% of bone tissue. It is mainly composed of type I collagen fibers that bind to each other in a triple helix structure [19]. In this study, the hydrogen relative concentration reflects primarily the protein content of the

bone matrix because fat and most of the water were eliminated from the specimens during the bone powder preparation, and the NMR spectrum permits exclusion of any residual fat signal.

^{1}H to ^{31}P cross-polarization measurement permits observing ^{31}P spectra when the ^{31}P spins are dilute (and the signal weak), but more importantly for the present measurements, it yields ^{31}P spectra predominantly from regions within the bone nanocrystals which are hydrogen-rich (generally in the surface regions of the nanocrystals). Thus, the four types of NMR spectra provide separate, though complementary, information.

Statistical analysis:

The statistical analysis was performed using SPSS 22.0 (SPSS Inc, Chicago, IL, USA), G*power 3.0.10 (Universität Kiel, Germany) and Origin Pro 8.0 (OriginLab Corporation, Northampton, USA) software. Mean values were presented with their corresponding standard deviations. The distribution of continuous variables was analyzed using Q-Q plots and the Shapiro–Wilk test. Differences between the two study groups were analyzed using a multivariate analysis of variance. Differences between groups were considered significant when two-tailed P values were < 0.05. Power analyses were performed using the Wilcoxon-Mann-Whitney test for two groups or a two-tailed post-hoc t-test for two independent means with an α-error probability of 0.05. Correlations between different continuous variables were adjusted to age, BMI and BV/TV using a linear regression model.

Results:

Demographic

A total of 84 femoral heads were collected during the study period, 11 were excluded, and 73 fulfilled our inclusion criteria (i.e., 31 hip fractures and 42 cases of hip osteoarthritis). The average age of the individuals that sustained a hip fracture was 79.6 years ± 10.1, whereas the mean age of patients with hip osteoarthritis was 64.38 years ± 10.3 (p=<0.001). The male-female ratio for patients with hip fractures and hip osteoarthritis was 0.34, and 1.21, respectively, (p=0.01). Individuals who suffered a hip fracture had a lower BMI compared with patients who had hip osteoarthritis (25.7 ±3.7 and 28.48 ± 3.9, respectively) (p=0.01). The smoking and non-smoking ratios for fractured patients and osteoarthritis patients were 0.35 and 0.68 respectively, (p=0.15). The mean age-factored Charlson comorbidity score for patients with hip fractures was 5.27 ± 1.98, compared to 2.82 ± 1.47 in patients with osteoarthritis (p=<0.001) (Table 1).

Bone densitometry:

The mean BMD in the osteoarthritis group (0.39 g/cm^2 ± 0.10) was higher than in hip fracture patients [0.28 g/cm^2 ± 0.05; p=0.002, power 99.9%]. The BMC was 0.18 g/cm ± 0.08 in individuals with osteoarthritis and 0.13 g/cm ± 0.05 in hip fracture patients. There were no significant differences in the T area between the hip fracture and osteoarthritis groups (Table 2).

Micro-computed tomography (µ-CT):

The BV/TV was higher in the osteoarthritis group 28.6% ± 10.5 than in the hip fracture group 20.3% ± 6.6 patients (p= 0.026; power 99.2%). The Tb.N was also higher in individuals with osteoarthritis 2.58 ± 1.57 than in patients with hip fractures 1.5 ± 0.79 (p=0.002; power 99.4%).

Moreover, the Tb.Sp was lower in the osteoarthritis group 0.42 ± 0.23 than in the hip fracture group 0.58 ± 0.28 (p=0.036; power 79.3%). No significant differences were found between the two groups regarding the Tb.Th (0.18 ± 0.02 in the hip fracture group vs. 0.13 ± 0.04 in osteoarthritis group, p=0.156) (Table 2).

X-ray powder diffraction:

There were no differences between the two groups involving the HA c-axis and a-axis (Table 2).

Solid-state magic-angle-spinning (MAS) nuclear magnetic resonance (NMR) spectroscopy:

No significant differences were found between the two groups, regarding hydrogen or phosphorus concentration measured by NMR spectroscopy (Table 2).

Correlations between bone mineral density and other structural features:

In the hip osteoarthritis group, BMD was strongly correlated with BV/TV (r=0.689, p=<0.001), and moderately correlated with Tb.N (r= 0.664; p=<0.001). BMD was negatively correlated with Tb.Sp (-0.561, p=<0.001), and ^{1}H concentration (-0.580, p=<0.001). A crude negative correlation was also observed between ^{1}H concentration and 31 P single pulse with proton decoupling (-0.535, p=<0.001). No correlations were observed between BMD and the length of the HA crystals on both the c-axis and a -axis in the hip osteoarthritis group.

In the hip fracture group, no correlations were found between BMD and BV/TV, Tb.Sp , Tb.Th, Tb.N, Tb. PF, hydrogen or phosphorus concentration, and HA crystal a-axis and c-axis. (Table 3) (Figures 2 and 3).

Discussion:

Bone microstructure:

In this study, we observed that patients who suffered a hip fracture had a higher Tb.Sp, lower Tb.N, and overall a lower BV/TV compared with patients with osteoarthritis. These results are in concordance with previous reports in the literature which suggest that compared with subjects with hip osteoarthritis, patients with hip fractures may suffer a deterioration in trabecular bone architecture [20–22]. A previous research comparing the microstructural features of trabecular and cortical bone between patients with hip fractures and osteoarthritis, reported that the cortical thinning, and the loss of the trabecular bone mass and connectivity could play a significant role in skeletal fragility in hip fractures [20]. The study also showed that the spatial orientation of the trabeculae differed between these two groups [20]. Another study compared the 2D and 3D bone microarchitecture of the femoral neck in postmenopausal women using high resolution peripheral quantitative tomography and histomorphometry. The 3D methods revealed an alteration of trabecular and cortical bone in hip fractures compared with osteoarthritis [21]. Moreover, a previous study performed by our team, in which we analyzed the femoral head 3D structure in hip fracture patients and subjects with hip osteoarthritis, revealed that the mean intercept length anisotropy was higher in the hip fracture group, whereas the osteoarthritis group had a higher connectivity density per unit volume than the hip fracture group [23]. Another cross-sectional study compared the mechanical and microstructural features of the femoral head in 17 postmenopausal women who underwent surgery for hip fracture or osteoarthritis. Significant differences were found in bone volume fraction (BV/TV) and trabecular thickness between the two groups [22].

316 On the other hand, research has suggested that the trabecular microstructure could act as an
317 independent factor contributing to bone strength [3–5]. In a study performed on middle aged men
318 with osteopenia, no differences were found in the BV/TV between individuals with vertebral
319 fractures and those who did not sustain fractures [3]. However, the authors of this study observed
320 higher trabecular connectivity and Tb.N in patients without vertebral fractures [3]. In a
321 comparative study analyzing the differences between cancellous bone in patients with hip
322 fractures and cadaveric controls, Ciarelli et al, reported that controls had a higher Tb.N and
323 connectivity than patients with hip fractures. However, as in our study, no differences were
324 found between the two groups regarding the trabecular thickness [5]. Another report analyzed 21
325 cadaveric bone samples using μCT system, digital topological analysis and μCT-based finite
326 element models. The study observed that the trabecular microarchitecture could also affect the
327 modulus of elasticity of trabecular bone [4]. All the previous mentioned studies highlight the
328 important contribution of the trabecular microstructure, including the trabecular number,
329 connectivity and anisotropy, on the mechanical properties of trabecular bone [3–5].

330 *Bone mineral density:*

331 We observed that individuals who suffered a hip fracture had a lower BMD than patients with
332 osteoarthritis. Previous reports have postulated that osteoarthritis and osteoporosis could be
333 inversely related conditions, as patients with early osteoarthritis may present increases in BMD
334 [24, 25]. However, the risk of suffering an osteoporotic fracture does not seem to decrease in
335 patients with osteoarthritis despite having higher BMD values [26]. This could involve other
336 factors not related to bone structure, such as postural instability and muscle strength. Low BMD
337 at the lumbar spine has also been found to be associated with a lower incidence of knee

osteoarthritis although it does not seem to stop the progression of knee osteoarthritis [26]. Nevertheless, the inverse relation between osteoporosis and osteoarthritis remains unclear.

In this study, the BMD was not correlated to BV/TV, Tb.N, and Tb.Sp in the hip fracture group. These findings are in concordance with recent research which analyzed the femoral heads in 16 patients who underwent hip arthroplasty [27]. Interestingly, in our study we did found a correlation between BMD and BV/TV, Tb.N, and Tb.Sp, in the osteoarthritis group. These findings suggest that DXA could be a useful method to estimate other architectural features of bone in patients with high bone densities, but not in subjects with low bone mineral densities. Therefore, patients with similar low bone densities could have significant microstructural differences. This could explain why the fracture predictive value of DXA scan decreases with age as BMD progressively declines [28, 29].

Hydroxyapatite crystals:

In this study, no differences were found between the two groups regarding the HA crystal c-axis and a-axis size. The relation between the mineral features of bone and its mechanical properties is poorly understood. HA crystals are arranged between collagen fibrils in bone. The size of these crystals determines the surface area where mineral-collagen interactions occur [30]. Longer HA crystals could increase the interaction surface and affect the mobility of the collagen molecules decreasing the overall tissue ductility. Pathologies known to enlarge the HA crystal size in animal studies (i.e., ovariectomized mice, rachitic rats, and osteopontin-null mice) have been found to increase bone fragility, ductility , and brittleness [30] . Nevertheless, conditions which decrease the crystal size (i.e., Osteogenesis imperfecta mice, hypophosphatemic mice, osteopetrotoc rats) have also been found to have a detrimental effect on the mechanical

properties of bone causing brittleness and reduced ductility [30] [31, 32]. This relation between mechanical properties and the grain size of poly crystalline materials is well explained by the Hall-Petch model that stipulates that above a critical crystal size an inverse correlation exists between material toughness and crystal size while this relation is reversed when the crystal size falls beneath the optimal critical size. This, alongside with our results and the previous literature would indicate that bone probably has an optimal crystal size consisting of a mixture of small (recently formed) and larger crystals and deviations beneath or above this crystal size would result in inferior mechanical properties. [30, 33, 34]. Although, the HA crystal size which carries the optimal mechanical properties in bone is still unknown [31].

Some animal and human studies have found that osteoporosis is associated with larger HA crystals compared to controls [30, 35]. In osteoporosis, bone turnover is accelerated [30, 35], as there is increased osteoclastic activity and [36] an overall decreased osteoblastic activity and less formation of new HA crystals. Subsequently, this could favor the predominance of older and larger HA crystals. In osteoarthritis , there is an early increase in bone remodeling and bone loss, followed by a slower turnover which leads to densification of the subchondral bone [37]. Two different groups of osteoblasts have been differentiated in osteoarthritis: low osteoarthritis osteoblasts, which present decreased OPG expression,increased in RANKL secretion, and probably induce bone resorption; and high osteoarthritis osteoblasts, which present increased OPG production and reduced RANKL expression, and may favor bone formation [38]. The latter group could result in a lower osteoclastic activity and therefore in the accumulation of more mature and larger HA crystals. Nevertheless, the specific mechanisms by which bone remodeling may influence the HA crystal size in osteoporosis and osteoarthritis are still unknown. However,

as mentioned above, both conditions have the potential to form larger HA crystals as a result of a decreased bone formation in osteoporosis and osteoclastic inhibition in osteoarthritis [35]. This could be a possible explanation to why in this study no HA crystal size differences were found between the two groups.

On the other hand, in this study we only analyzed trabecular bone, which is less dense than cortical bone and enamel. Previous research has shown that the bone strength was strongly related to the trabecular microstructural features, whereas the strength of cortical bone was more related with the total cortical bone volume [39]. Moreover, multiple studies have shown that cortical porosity, a microstructural measure of cortex plays an important role in bone strength [40] [41]. Perhaps, the HA crystal size at the nanostructural level could have a more significant influence on cortical bone strength, were porosity and total cortical bone volume play more determinant roles.

The organic matrix:

No significant differences were found between the two groups, regarding the hydrogen content of trabecular bone. However, we observed a trend showing a higher relative phosphorus concentration with ^{31}P single pulse NMR spectroscopy in patients with osteoarthritis. The importance of the organic content in bone is evident in conditions such as osteogenesis imperfecta, some forms of osteoporosis, and osteomalacia (impaired mineralization). In osteogenesis imperfecta mutations in the COL1A1 and COL1A2 genes result in the formation thinner collagen fibrils, and consequently the formation of excessively brittle bone [42]. In

idiopathic osteoporosis and postmenopausal women, there is increasing evidence suggesting that a high remodeling rate could be associated with decreased bone mineralization and subsequently reduced bone stiffness. In addition, higher bone turnover rates could alter the content of collagen crosslinks [43]. Conditions that may result in impaired bone mineralization (osteomalacia, or insufficient mineral with respect to the amount of matrix), such as chronic kidney disease, calcium malabsorption in the small intestine, vitamin-D deficiency or inadequate ultraviolet exposure of the skin, can lead to bone pain, skeletal fragility and distortion, and microfractures. Moreover, recent research has found that the cross-link profile of bone collagen correlates with bone fracture toughness and strength [44]. The orientation of collagen fibers is another factor involved in bone strength. Accordingly, the strength of bone tissue is higher in the direction of physiological loading that corresponds to the orientation of osteons in the cortical bone [45].

Research has shown that bone hardness is strongly correlated to mineralization, but the organic matrix also accounts for a significant part of its variance [46]. A previous report observed that long-term running in dogs significantly reduced the vertebral BMD, and lead to the reorganization of the collagen fibers without changing the mechanical properties of bone [43]. Another study, revealed that COL1A1 Sp1 polymorphism could be associated with both bone strength and BMD [47]. These findings suggest that the bone strength depends on the balance between the organic and mineral content of bone, and that the collagen matrix could act as an important independent factor in bone strength.

On the other hand, we observed an inverse correlation between the quantity of the organic matrix in the osteoarthritis group measured as ^{1}H, and both BMD and 31P single pulse with proton decoupling. These last two measurements reflect the bone mineral content. In addition to the

physical and biochemical changes in articular cartilage that occur in osteoarthritis, the subchondral bone often undergoes morphological changes as a result of an abnormal remodeling, turnover and mineralization [48]. The inverse correlation between BMD and the organic matrix content is a clear confirmation of the relative demineralization that is known to occur in osteoarthritis [49]. This correlation was not observed in the osteoporotic hip fracture group, no such effect is generally known to occur in osteoporosis.

Strengths and limitations:

To the best of our knowledge this is the first study to show that the HA crystal size in trabecular bone does not differ between patients with osteoarthritis and individuals with osteoporotic fractures. Moreover, this study was the first to identify an inverse relation between BMD and the quantity of the organic matrix in humans using solid-state NMR spectroscopy. In addition, this study highlights the limitations of DXA scan in the estimation of trabecular bone structural features in patients with low bone densities. This study has a relatively large sample size compared with previous reports, and our statistical analyses were adjusted to eliminate potential confounders using linear regression models or multivariable analyses of variance. However, this work has several limitations. We did not include a mechanical analysis of the samples which would have provided valuable information on the relation between the different structural properties of bone and mechanical bone strength. In addition, we only included a relatively limited age range, confined only to elderly individuals who underwent joint replacement surgery; therefore, the bone features that have been observed in this study can only be extrapolated to an elderly population.

In this study, hip fracture patients were relatively older compared with osteoarthritis patients. The structural features of bone change with age, as part of the natural aging process. Previous research has shown that BMD and the organic bone content progressively decrease with age [50, 51]. Therefore, age could have acted as an independent confusion factor in the present study. However, to decrease a possible age-related confusion bias, our linear regression models and multivariable analyses of variances were adjusted to age-factored CCI. Finally, our study was also limited to the analysis of the cancellous femoral head bone and it did not include tests involving the lumbar spine or cortical bone.

Conclusions:

Individuals with osteoarthritis have a higher BMD, BV/TV, and trabecular number that patients who suffered hip fractures. Moreover, the HA crystal size in trabecular bone does not differ between patients with osteoarthritis and individuals with osteoporotic fractures. In the osteoarthritis group, BMD was correlated with BV/TV, Tb.N, and Tb.Sp. However, BMD was not correlated to BV/TV, Tb.N, and Tb.Sp in the hip fracture group. This could explain why the fracture predictive value of BMD decreases in older populations with lower BMDs, as patients with similar low densities could have significant microstructural differences. This study was also the first to identify an inverse relation between BMD and the quantity of the organic matrix in humans using solid-state NMR spectroscopy. However, this correlation was only found in patients with osteoarthritis.

References:

1. Reznikov N, Steele JAM, Fratzl P, Stevens MM (2016) A materials science vision of extracellular matrix mineralization. Nature Reviews Materials 1:16041. https://doi.org/10.1038/natrevmats.2016.41

2. Seeman E, Delmas PD (2006) Bone quality--the material and structural basis of bone strength and fragility. N Engl J Med 354:2250–2261. https://doi.org/10.1056/NEJMra053077

3. Legrand E, Chappard D, Pascaretti C, et al (2000) Trabecular Bone Microarchitecture, Bone Mineral Density, and Vertebral Fractures in Male Osteoporosis. Journal of Bone and Mineral Research 15:13–19. https://doi.org/10.1359/jbmr.2000.15.1.13

4. Liu XS, Sajda P, Saha PK, et al (2006) Quantification of the Roles of Trabecular Microarchitecture and Trabecular Type in Determining the Elastic Modulus of Human Trabecular Bone. J Bone Miner Res 21:1608–1617. https://doi.org/10.1359/jbmr.060716

5. Ciarelli TE, Fyhrie DP, Schaffler MB, Goldstein SA (2000) Variations in Three-Dimensional Cancellous Bone Architecture of the Proximal Femur in Female Hip Fractures and in Controls. Journal of Bone and Mineral Research 15:32–40. https://doi.org/10.1359/jbmr.2000.15.1.32

6. Cummings SR, Browner W, Cummings SR, et al (1993) Bone density at various sites for prediction of hip fractures. The Lancet 341:72–75. https://doi.org/10.1016/0140-6736(93)92555-8

7. Venkateswarlu K, Chandra Bose A, Rameshbabu N (2010) X-ray peak broadening studies of nanocrystalline hydroxyapatite by Williamson–Hall analysis. Physica B: Condensed Matter 405:4256–4261. https://doi.org/10.1016/j.physb.2010.07.020

8. Klinowski J (2005) New Techniques in Solid-State NMR. Springer-Verlag, Berlin Heidelberg

9. Kaflak A, Chmielewski D, Górecki A, Kolodziejski W (1998) Kinetics of 1H --> 31P cross-polarization in human trabecular bone. Solid State Nucl Magn Reson 10:191–195. https://doi.org/10.1016/S0926-2040(97)00085-4

10. Cao H, Nazarian A, Ackerman JL, et al (2010) Quantitative 31P NMR spectroscopy and 1H MRI measurements of bone mineral and matrix density differentiate metabolic bone diseases in rat models. Bone 46:1582–1590. https://doi.org/10.1016/j.bone.2010.02.020

11. Wu Y, Ackerman JL, Strawich ES, et al (2003) Phosphate ions in bone: identification of a calcium–organic phosphate complex by 31 P solid-state NMR spectroscopy at early stages of mineralization. Calcified tissue international 72:610–626

12. Roffman CE, Buchanan J, Allison GT (2016) Charlson Comorbidities Index. Journal of Physiotherapy 62:171. https://doi.org/10.1016/j.jphys.2016.05.008

13. Ghadimi E, Eimar H, Marelli B, et al (2013) Trace elements can influence the physical properties of tooth enamel. SpringerPlus 2:499. https://doi.org/10.1186/2193-1801-2-499

14. Hanlie H, Liyun T, Tao J (2006) The crystal characteristics of enamel and dentin by XRD method. J Wuhan Univ Technol-Mat Sci Edit 21:9. https://doi.org/10.1007/BF02861458

15. Xue J, Zhang L, Zou L, et al (2008) High-resolution X-ray microdiffraction analysis of natural teeth. J Synchrotron Rad, J Synchrotron Radiat 15:235–238. https://doi.org/10.1107/S0909049508003397

16. Dal Sasso G, Asscher Y, Angelini I, et al (2018) A universal curve of apatite crystallinity for the assessment of bone integrity and preservation. Scientific Reports 8:1–13. https://doi.org/10.1038/s41598-018-30642-z

17. Wu Y, Glimcher MJ, Rey C, Ackerman JL (1994) A Unique Protonated Phosphate Group in Bone Mineral Not Present in Synthetic Calcium Phosphates: Identification by Phosphorus-31 Solid State NMR Spectroscopy. Journal of Molecular Biology 244:423–435. https://doi.org/10.1006/jmbi.1994.1740

18. Ramanathan C, Ackerman JL (1997) ADRF differential cross polarization spectroscopy of synthetic calcium phosphates and bone mineral. J Magn Reson 127:26–35. https://doi.org/10.1006/jmre.1997.1173

19. Clarke B (2008) Normal bone anatomy and physiology. Clin J Am Soc Nephrol 3 Suppl 3:S131-139. https://doi.org/10.2215/CJN.04151206

20. Blain H, Chavassieux P, Portero-Muzy N, et al (2008) Cortical and trabecular bone distribution in the femoral neck in osteoporosis and osteoarthritis. Bone 43:862–868. https://doi.org/10.1016/j.bone.2008.07.236

21. Boutroy S, Vilayphiou N, Roux J-P, et al (2011) Comparison of 2D and 3D bone microarchitecture evaluation at the femoral neck, among postmenopausal women with hip fracture or hip osteoarthritis. Bone 49:1055–1061. https://doi.org/10.1016/j.bone.2011.07.037

22. Zhang Z-M, Li Z-C, Jiang L-S, et al (2010) Micro-CT and mechanical evaluation of subchondral trabecular bone structure between postmenopausal women with osteoarthritis and osteoporosis. Osteoporos Int 21:1383–1390. https://doi.org/10.1007/s00198-009-1071-2

23. Reznikov N, Alsheghri AA, Piché N, et al (2020) Altered topological blueprint of trabecular bone associates with skeletal pathology in humans. Bone Reports 12:100264. https://doi.org/10.1016/j.bonr.2020.100264

24. Hart DJ, Mootoosamy I, Doyle DV, Spector TD (1994) The relationship between osteoarthritis and osteoporosis in the general population: the Chingford Study. Ann Rheum Dis 53:158–162

25. Shen Y, Zhang Z-M, Jiang S-D, et al (2009) Postmenopausal women with osteoarthritis and osteoporosis show different ultrastructural characteristics of trabecular bone of the femoral head. BMC Musculoskeletal Disorders 10:35. https://doi.org/10.1186/1471-2474-10-35

26. Im G-I, Kim M-K (2014) The relationship between osteoarthritis and osteoporosis. J Bone Miner Metab 32:101–109. https://doi.org/10.1007/s00774-013-0531-0

27. Peng J, Zhou Y, Min L, et al (2014) [Analysis of correlation between trabecular microstructure and clinical imaging parameters in fracture region of osteoporotic hip]. Zhongguo Xiu Fu Chong Jian Wai Ke Za Zhi 28:576–580

28. Kanis JA, Johnell O, Oden A, et al (2000) Prediction of fracture from low bone mineral density measurements overestimates risk. Bone 26:387–391. https://doi.org/10.1016/S8756-3282(00)00238-6

29. Johnell O, Kanis JA, Oden A, et al (2005) Predictive value of BMD for hip and other fractures. J Bone Miner Res 20:1185–1194. https://doi.org/10.1359/JBMR.050304

30. Adele Boskey (2003) Bone mineral crystal size. Osteoporos Int 14 Suppl 5:S16-20; discussion S20-21. https://doi.org/10.1007/s00198-003-1468-2

31. Bala Y, Farlay D, Boivin G (2013) Bone mineralization: from tissue to crystal in normal and pathological contexts. Osteoporos Int 24:2153–2166. https://doi.org/10.1007/s00198-012-2228-y

32. Bouxsein ML (2005) Determinants of skeletal fragility. Best Pract Res Clin Rheumatol 19:897–911. https://doi.org/10.1016/j.berh.2005.07.004

33. Wang N, Wang Z, Aust KT, Erb U (1995) Effect of grain size on mechanical properties of nanocrystalline materials. Acta Metallurgica et Materialia 43:519–528. https://doi.org/10.1016/0956-7151(94)00253-E

34. Eimar H, Ghadimi E, Marelli B, et al (2012) Regulation of enamel hardness by its crystallographic dimensions. Acta Biomaterialia 8:3400–3410. https://doi.org/10.1016/j.actbio.2012.06.002

35. Noor Z, Sumitro SB, Hidayat M, et al (2016) Assessment of microarchitecture and crystal structure of hydroxyapatite in osteoporosis. Universa Medicina 30:29–35. https://doi.org/10.18051/UnivMed.2011.v30.29-35

36. Guido G, Scaglione M, Fabbri L, Ceglia MJ (2009) The “osteoporosis disease.” Clin Cases Miner Bone Metab 6:114–116

37. Burr DB, Gallant MA (2012) Bone remodelling in osteoarthritis. Nature Reviews Rheumatology 8:665–673. https://doi.org/10.1038/nrrheum.2012.130

38. Maruotti N, Corrado A, Cantatore FP (2017) Osteoblast role in osteoarthritis pathogenesis. J Cell Physiol 232:2957–2963. https://doi.org/10.1002/jcp.25969

39. Ito M, Nishida A, Koga A, et al (2002) Contribution of trabecular and cortical components to the mechanical properties of bone and their regulating parameters. Bone 31:351–358. https://doi.org/10.1016/S8756-3282(02)00830-X

40. Samelson EJ, Broe KE, Xu H, et al (2019) Cortical and trabecular bone microarchitecture as an independent predictor of incident fracture risk in older women and men in the Bone Microarchitecture International Consortium (BoMIC): a prospective study. Lancet Diabetes Endocrinol 7:34–43. https://doi.org/10.1016/S2213-8587(18)30308-5

41. Vilayphiou N, Boutroy S, Sornay-Rendu E, et al (2016) Age-related changes in bone strength from HR-pQCT derived microarchitectural parameters with an emphasis on the role of cortical porosity. Bone 83:233–240. https://doi.org/10.1016/j.bone.2015.10.012

42. Kirsch E, Krieg T, Remberger K, et al (1981) Disorder of collagen metabolism in a patient with osteogenesis imperfecta (lethal type): increased degree of hydroxylation of lysine in collagen types I and III. Eur J Clin Invest 11:39–47. https://doi.org/10.1111/j.1365-2362.1981.tb01763.x

43. Viguet-Carrin S, Garnero P, Delmas PD (2006) The role of collagen in bone strength. Osteoporos Int 17:319–336. https://doi.org/10.1007/s00198-005-2035-9

44. McNerny EMB, Gong B, Morris MD, Kohn DH (2015) Bone fracture toughness and strength correlate with collagen cross-link maturity in a dose-controlled lathyrism mouse model. J Bone Miner Res 30:455–464. https://doi.org/10.1002/jbmr.2356

45. Heřt J, Fiala P, Petrtýl M (1994) Osteon orientation of the diaphysis of the long bones in man. Bone 15:269–277. https://doi.org/10.1016/8756-3282(94)90288-7

46. Boivin G, Bala Y, Doublier A, et al (2008) The role of mineralization and organic matrix in the microhardness of bone tissue from controls and osteoporotic patients. Bone 43:532–538. https://doi.org/10.1016/j.bone.2008.05.024

47. Uitterlinden AG, Burger H, Huang Q, et al (1998) Relation of alleles of the collagen type Ialpha1 gene to bone density and the risk of osteoporotic fractures in postmenopausal women. N Engl J Med 338:1016–1021. https://doi.org/10.1056/NEJM199804093381502

48. Li G, Yin J, Gao J, et al (2013) Subchondral bone in osteoarthritis: insight into risk factors and microstructural changes. Arthritis Res Ther 15:223. https://doi.org/10.1186/ar4405

49. Grynpas MD, Alpert B, Katz I, et al (1991) Subchondral bone in osteoarthritis. Calcif Tissue Int 49:20–26. https://doi.org/10.1007/BF02555898

50. Sanchez-Siles JM, Tamimi-Mariño I, Cortes ARG, et al (2020) Age related changes in the bone microstructure in patients with femoral neck fractures. Injury. https://doi.org/10.1016/j.injury.2020.02.014

51. Burger H, van Daele PLA, Algra D, et al (1994) The association between age and bone mineral density in men and women aged 55 years and over: The Rotterdam Study. Bone and Mineral 25:1–13. https://doi.org/10.1016/S0169-6009(08)80203-6

Legends:

Figure 1: A. The region where the bone samples were harvested during standard total hip and partial hip replacement procedures. B. A 1.0 cm Ø x 1.5 cm cylindrical bone sample. The

626 selected region of interest on an anteroposterior x-ray view. Micro-computed tomography axial
627 cut of the femoral head samples: C and E hip fracture; D and F hip osteoarthritis.

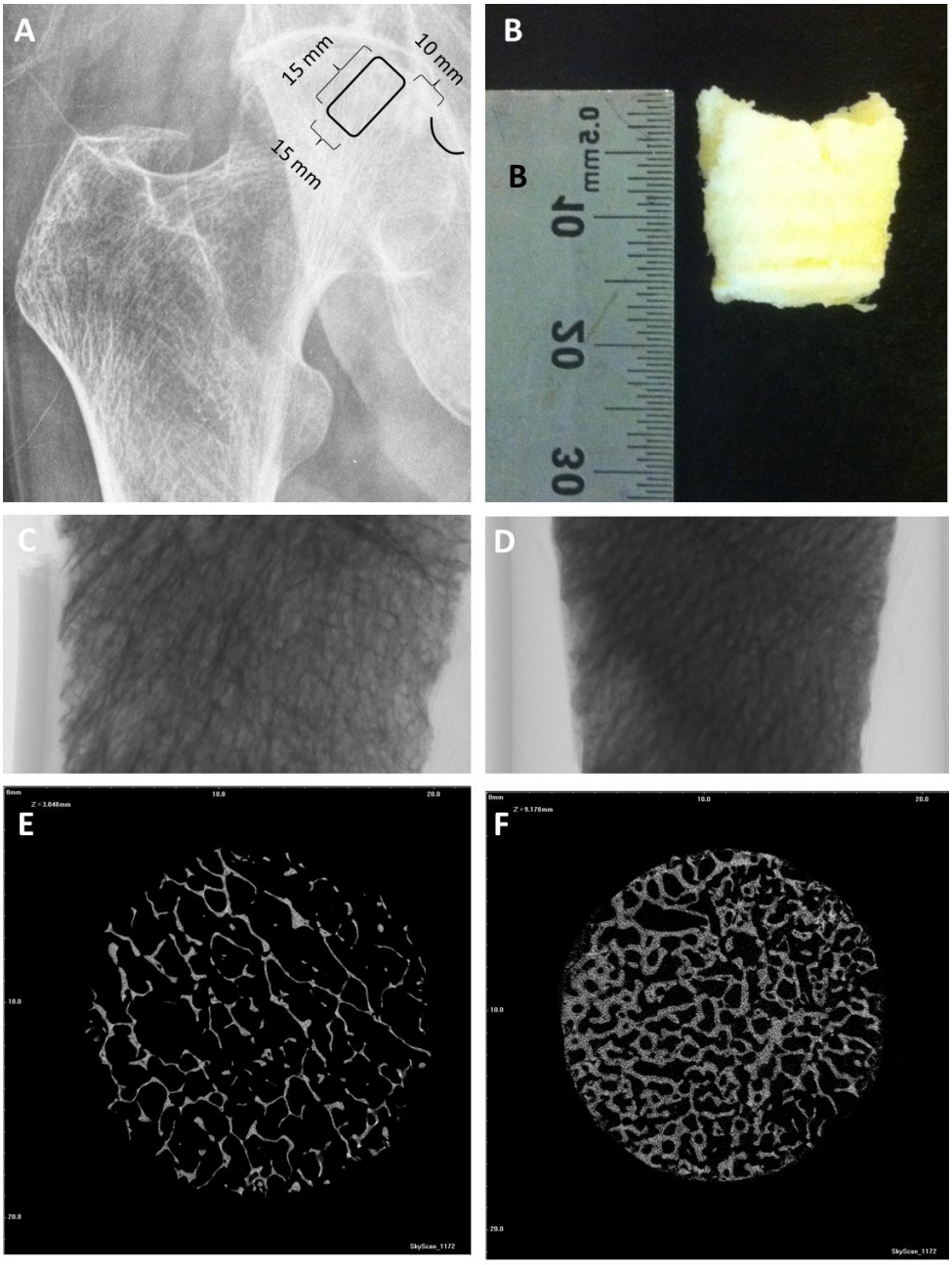

628

Figure 2: Correlation between bone mineral density and other structural features on µ-CT scan.

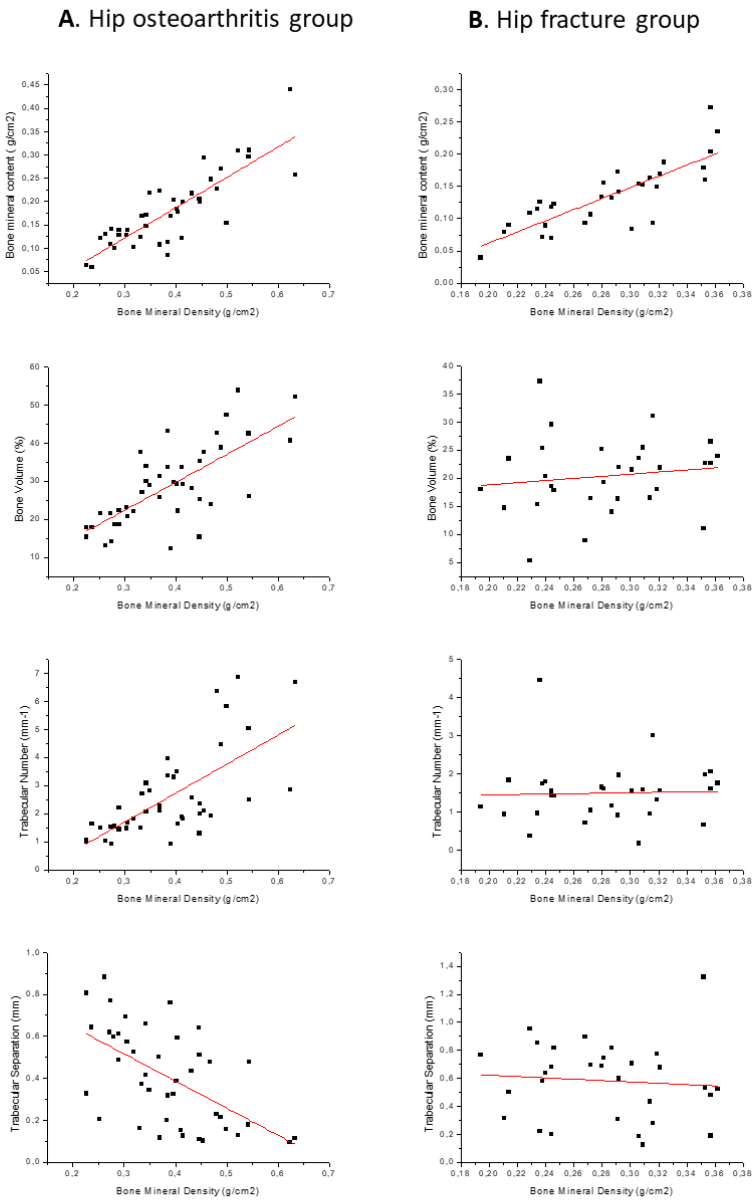

Figure 3: Correlation between bone mineral density and hydroxyapatite crystal size and hydrogen content from single pulse proton solid-state magic-angle-spinning NMR spectroscopy.

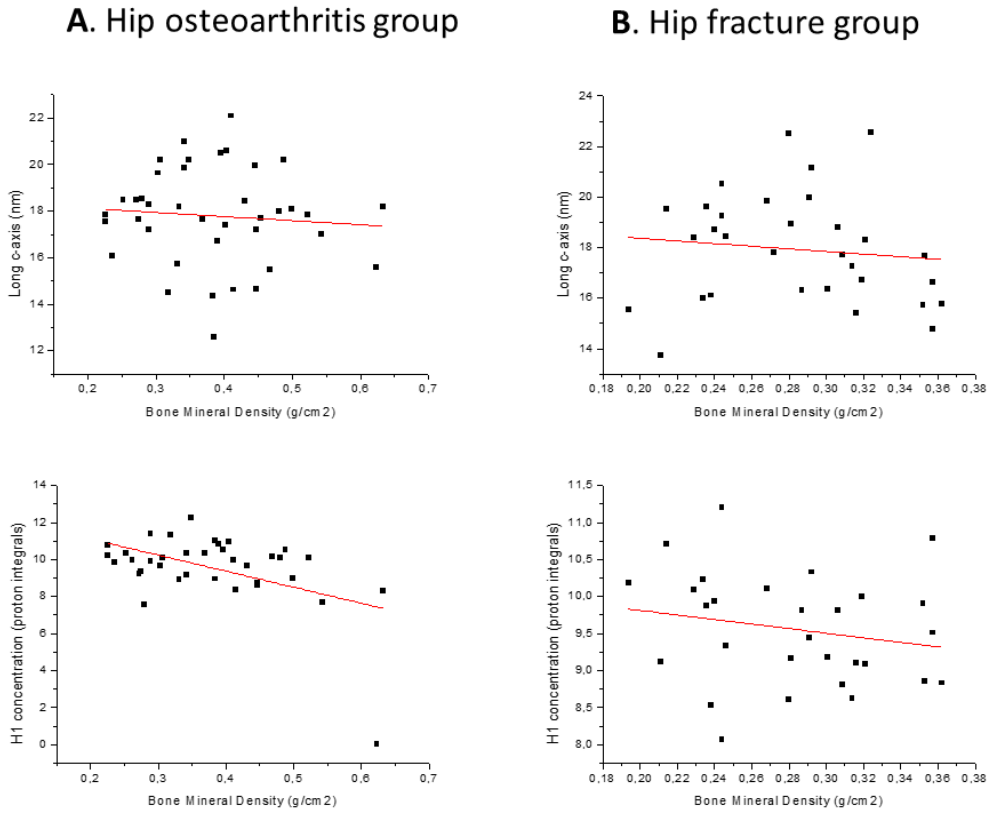

639

Table 1. Demographic features of the study group

Characteristics	Hip fracture (n= 31)	Hip osteoarthritis (n=42)	P values
Age, y	79.6 ± 10.1	64.4 ± 10.3	<0.001*
Sex			
Men	8 (25.8)	23 (54.8)	0.01*
Women	23 (74.2)	19 (45.2)	
Smoking status			
Yes	8 (25.8)	17 (40.5)	0.15
No	23 (74.2)	25 (59.5)	
Body mass index [a]	25.7 ±3.7	28.48 ± 3.9	0.01*
Operated Side			
Right	14 (45.2)	14 (66.7)	0.06*
Left	17 (54.8)	28 (33.3)	
Alcohol abuse			
Yes	2 (6.5)	4 (9.5)	0.49
No	29 (93.5)	38 (90.5)	
CCI	5.27 ±1.98	2.82 ± 1.47	<0.001*

Data are presented as No. (%) or mean ± standard deviation.
Abbreviations: CCI, age-factored Charlson comorbidity score.
[a] Measured as weight in kilograms divided by the square of height in meters.
*Statistically significant results
Student T, Chi square, Mann-Whitney U

640

641

642

643

644

645

646

647

648

649

Table 2. Multivariable analysis of variance adjusted to bone volume fraction, and body mass index and Age-factored-Charlson´s comorbidity index. Structural features of trabecular bone, hip fracture vs. osteoarthritis (Micro-computed tomography, dual-energy x-ray absorptiometry, x-ray diffraction and Solid-state magic-angle-spinning nuclear magnetic resonance spectroscopy).

Characteristics	**Hip fracture (n= 31)**	**Hip osteoarthritis (n=42)**	**Crude P value**	**Adjusted P values**
BV/TV (%)	20.37 ± 6.6	28.62 ± 10.51	0.001*	0.026*
Tb.Sp (mm)	0.58 ± 0.28	0.42 ± 0.23	0.005*	0.036*
Tb.Th (mm)	0.18 ± 0.021	0.13 ± 0.037	0.043*	0.156
Tb.N (mm^{-1})	1.5 ± 0.79	2.58 ± 1.57	0.000*	0.002*
Tb.Pf (mm^{-1})	-0.49 ± 20.59	-9.32 ± 25.62	0.072	0.101
BMD (g/cm^2)	0.28 ± 0.05	0.39 ± 0.115	0.000*	0.002*
BMC (g/cm^2)	0.13 ± 0.05	0.18 ± 0.08	0.020*	0.195*
B area (cm^2)	4.62 ± 1.18	4.51± 1.13	0.492	0.442
T area (cm^2)	5.05 ± 1.24	4.83 ± 1.2	0.226	0.337
HA c-axis[a] (nm)	17.1 ± 1.8	17.2 ± 2.2	0.901	0.775
HA a-axis[a] (nm)	8.1 ± 0.9	7.96 ± 1.3	0.675	0.853
Hydrogen concentration[b]	0.956 ± 0.08	0.983 ±0.11	0.232	0.325
Phosphorus concentration[c]	6.90 ± 1.9	7.41 ± 1.8	0.206	0.318
Phosphorus	7.18 ± 2.0	7.66 ± 2.1	0.377	0.494

concentration[d]				
Phosphorus concentration[e]	1.2 ± 0.3	1.74 ± 1.5	0.269	0.141

Abbreviations: BV/TV, bone volume fraction; Tb.Pf, trabecular pattern factor; Tb.N, trabecular number; Tb.Sp, trabecular separation; Tb.Th, trabecular thickness; BMD, bone mineral density; BMC, bone mineral content.

Data are presented as mean ± standard deviation.

*Statistically significant results

[a]Hydroxyapatite crystals

[b]Relative intensity of integrated signal in single pulse ^{1}H MAS NMR spectroscopy

[c]Relative intensity of integrated signal in single pulse ^{31}P MAS NMR spectroscopy

[d]Relative intensity of integrated signal in single pulse ^{31}P MAS NMR spectroscopy with ^{1}H decoupling

[e]Relative intensity of integrated signal in ^{1}H-^{31}P cross polarization PMAS NMR spectroscopy

650

651

652

Table 3 Correlation between Bone mineral density and other structural features on micro-computed tomography, dual-energy x-ray absorptiometry, x-ray diffraction and Solid-state magic-angle-spinning nuclear magnetic resonance spectroscopy

Characteristics	**Correlation coefficient R Hip fracture (n= 31)**		**Correlation coefficient R Hip osteoarthritis (n=42)**		**Correlation coefficient R (both groups, n=73)**	
	Crude	**Adjusted**	**Crude**	**Adjusted**	**Crude**	**Adjusted**
BV/TV (%)	0.138	0.112	0.720*	0.704*	0.694*	0.689*
Tb.Sp (mm)	-0.083	-0.035	-0.580*	-0.561*	-0.497*	-0.486*
Tb.Th (mm)	-0,049	-0.078	-0.360*	-0.295	-0.353*	-0.313*
Tb.N (mm^{-1})	0.034	0.080	0.679*	0.653*	0.661*	0.664*

Tb.Pf (mm^{-1})	0.174	0.239	-0.201	-0.108	-0.196	-0.152
BMC (g/cm^2)	0.819*	0.836*	0.843*	0.853*	0.845*	0.850*
HA c-axis[a] (nm)	-0.114	-0.464	-0.085	-0.084	-0.107	-0.136
HA a-axis[a] (nm)	-0.025	-0.084	-0.055	-0.065	-0.104	-0.099
Hydrogen concentration[b]	-0.201	-0.115	-0.478*	-0.580*	-0.385*	-0.494*
Phosphorus concentration[c]	-0.123	-0.068	0.011	-0.100	0.044	-0.010
Phosphorus concentration[d]	-0.052	-0.034	0.143	-0.045	0.131	-0.016
Phosphorus concentration[e]	-0.001	-0.058	0.062	0.050	0.138	0. 188

*Statistically significant

Abbreviations: BV/TV, bone volume fraction; Tb.Pf, trabecular pattern factor; Tb.N, trabecular number; Tb.Sp, trabecular separation; Tb.Th, trabecular thickness; BMC, bone mineral content; BMI , body mass index.

*Statistically significant results

[a]Hydroxyapatite crystals

[b]Relative intensity of integrated signal in single pulse ^{1}H MAS NMR spectroscopy

[c]Relative intensity of integrated signal in single pulse ^{31}P MAS NMR spectroscopy

[d]Relative intensity of integrated signal in single pulse ^{31}P MAS NMR spectroscopy with ^{1}H decoupling

[e]Relative intensity of integrated signal in ^{1}H-^{31}P CPMAS NMR spectroscopy

Linear regression analysis adjusted to age, BMI and BV/TV

653